



Trade Science Inc.

Nano Science and Nano Technology

An Indian Journal

Full Paper

NSNTAJ, 7(5), 2013 [179-188]

Structural, optical and thermal characterization of ZnO nanoparticles doped in PEO/PVA blend films

F.H.Abd El-Kader¹, N.A.Hakeem², I.S.Elashmawi^{2,3}, A.M.Ismail^{2*}

¹Physics Department, Faculty of Science, Cairo University, Giza, (EGYPT)

²Spectroscopy Department, Physics Division, National Research Center, Giza, (EGYPT)

³Physic Department, Faculty of Science, Taibah University, Al-Ula, (SAUDIA ARABIA)

E-mail : asmaanrc@yahoo.com

ABSTRACT

Solid polymer blend films based on PEO/PVA (50/50 wt/wt %) undoped and doped with different concentration of ZnO nanoparticles were prepared by using casting technique. Structural, optical and thermal studies were performed using Fourier transform infrared (FT-IR), X-ray diffraction (XRD), ultra violet - visible spectra (UV-VIS), scanning electron microscope (SEM), differential scanning calorimetry (DSC) and thermogravimetric analysis (TGA). IR absorption spectra and DSC thermograms indicate that the PEO/PVA undoped blend and doped with ZnO are immiscible. XRD and band tail energy data showed that the incorporation of nano-ZnO into the polymeric system causes decreasing the crystallinity of samples. The kinetic thermodynamic parameters such as activation energy, enthalpy, entropy and Gibbs free energy were evaluated from TG data using Coats – Redfern relation. SEM analysis indicate the change of the surface morphology of PEO/PVA/ZnO- nano particles.

© 2013 Trade Science Inc. - INDIA

KEYWORDS

Nanocomposites;
FT-IR;
X-ray diffraction;
Optical properties;
DSC;
TGA.

INTRODUCTION

Polyvinyl alcohol (PVA) polymers have attracted attention due to their variety of applications. PVA is a water soluble polymer which is important from an industrial view point. Some studies reveal that the optical and thermal properties of the PVA can be controlled by doping for different applications^[1,2]. Polyethylene oxide (PEO) is the most interesting base material because of it is high chemical and thermal stability^[3]. PEO is semi-crystalline polymer, possessing both amorphous and crystalline phases at room temperature.

Polymer blends often exhibit properties that are superior compared to the properties of each individual component polymer^[4]. Polymer nanocomposites have attracted a great deal of attention in recent years due to their exceptional properties^[5]. ZnO is an odd material with novel applications due to it's proper optical, electrical and thermal properties^[6,7]. Nano-ZnO is one of the multifunctional inorganic nanoparticles has drawn increasing attention in recent years due to it's many significant properties such as chemical stability, high catalysis activity and intensive ultraviolet and infrared absorption^[8-10]. In particular, the introduction of nano-ZnO

Full Paper

into polymeric matrix can enhance both mechanical and optical properties of the polymers due to a strong interfacial interaction between the organic polymer and the inorganic nanoparticles^[11]. Composites based on such nanoparticles can be widely utilised in coating, rubbers, plastics, sealants, fibers and other application. J. Lee et al.^[11] described the development of PEO/PVA/nano-ZnO film, then evaluated and optimized the effect of ZnO additive on some physical properties of the polyblend polymer.

The main purpose of this work was to achieve a deeper insight into the fundamental physical properties of PEO/PVA blend films doped with different concentration of ZnO nanoparticles. A systematic investigation on miscibility, thermal stability, structure, morphology and band tail property relationship of such nano-ZnO polyblend system are discussed using different tools and techniques.

EXPERIMENTAL WORK

Materials

Poly ethylene oxide (ACROS, New Jersey, USA) with M.W. \approx 900.000 and Poly vinyl alcohol (MP Biomedicals, Inc, France) with M.W. \approx 15.000 were used as a basic polymeric materials. Nano-powder of ZnO with a mean particles size <100 nm was supplied by SIGMA-ALDRICH, USA. All chemicals were used as received without any purification.

Preparation method

Equal quantity of PEO and PVA (50/50 wt/wt %) was dissolved in double distilled water separately and then the polymer blend solution was stirred continuously until a homogenous viscous liquid was formed. ZnO nanoparticles were dissolved in double distilled water also. The resulting solution of ZnO nanoparticles was added drop by drop to the polymer solution with mass fraction 0.5, 1.0, 2.5, 5.0 and 10 % wt. The resulting solution was cast to PEI Petri dishes and kept in a dry atmosphere at 70 °C about 48 hrs. After drying, the films were peeled from Petri dishes and kept in vacuum desiccators until uses.

Measurement techniques

FT-IR measurements were performed using

JASCO, FT/IR-6100 in the spectral range of 4000-400 cm^{-1} . X-ray diffractions were performed using Diano Corporation-USA equipped using Cu-K α radiation ($\lambda=0.1540$ nm, the tube operated at 30kV, Bragg's angle (2θ) in the range (5-50°). Ultraviolet-visible absorption spectra were measured in the wavelength region of 200-1000 nm using V-570 UV-VIS-NIR (JASCO, Japan) spectrophotometer. Scanning electron micrograph was performed using SEM (JEOL-JSM 6100), operating voltage at 30KV accelerating voltage. Differential scanning calorimetry of the prepared samples were carried out using (DSC-50, Shimadzu, Japan) with measuring temperature range from room temperature to 400°C and the heating rate was 10°C/min. The Thermogravimetric analysis (TGA) was used to characterize the decomposition and thermal stability of prepared samples by A Perkin-Elmer TGA-7. The mass of the samples amount (1-2.8 mg) was recorded while temperature is increase at a heating rate of 10°C/min and the samples heated from room temperature to 460 °C.

RESULTS AND DISCUSSION

Fourier transform infrared analysis (FT-IR)

FT-IR spectroscopy is an important tool to investigate multi-component systems, because it provides information on the specific groups found in the blend composition as well as the polymer-polymer interactions.

Figure 1 depicts the FT-IR spectra of PEO and PVA homopolymers and their blend sample of 50/50 (wt/wt %) PEO/PVA in the range 4000-400 cm^{-1} . The IR spectra of both PVA and PEO homopolymers seem to be consistent with that previously reported^[13,12-14]. The most important bands feature of these samples below 2000 cm^{-1} appears to be C=O stretching vibration at 1730 cm^{-1} and 1567 cm^{-1} , O-H bending vibration at 1328 cm^{-1} and C-O-C stretching vibration around 1100 cm^{-1} . However bands feature above 2000 cm^{-1} are intense and composition sensitive. They are the $\nu(\text{CH})$ stretching at 2884 cm^{-1} and $\nu(\text{OH})$ stretching at 3400 cm^{-1} . Whereas $\nu(\text{COC})$ stretching is present only in the spectrum of PEO but $\nu(\text{OH})$ and $\nu(\text{C=O})$ are present only in the spectrum of PVA^[12]. In general, the blend comprising the two compounds shows spectrum characteristic of both, but the vibrational bands characteriz-

ing each polymer are predominate.

In case of blend sample spectrum, the intensities of the absorption bands of $\nu(\text{OH})$, $\nu(\text{CH})$ and $\nu(\text{COC})$ stretching vibrations are change irregularly compared to their values in individual polymers, while their positions remains unaffected. Therefore intermolecular hydrogen bonding between PEO and PVA may not be significant at all^[12].

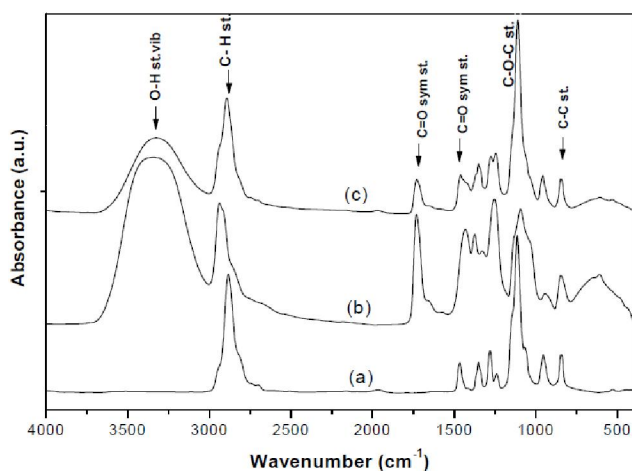


Figure 1 : FT-IR absorption spectra of (a) pure PEO, (b) pure PVA, (c) 50/50 (wt/wt. %) PEO/PVA blend sample.

Figure 2 shows IR spectra for PEO/PVA blend sample doped with 0.5, 1.0, 2.5, 5.0 and 10 wt. % of ZnO nanoparticles. From Figure 2 it can be seen that there is an increase in the absorption intensity of bands at 2936, 1730 and 1567 cm^{-1} with increasing the concentration of ZnO nanoparticles. In addition, the multiplicity and broadness of vibrational bands $\nu(\text{OH})$ and $\nu(\text{CH})$ increase with increasing ZnO content in blend sample. However, the new absorption bands appeared at ~ 600 and ~ 527 cm^{-1} are reflected the presence of nano-ZnO vibrational groups^[15]. These results indicate that a strong interaction occurred at the interface of ZnO nanoparticles which act as a filler with polyblend polymer matrix.

X-ray diffraction (XRD)

XRD analysis is very useful in knowing the structure of the polymeric materials. XRD patterns enable one to find out whether a material is crystalline or amorphous.

Figure 3 represents the X-ray diffraction of PEO/PVA blend films undoped and doped with different concentration of ZnO nanoparticles in the scanning range $5^\circ \leq 2\theta \leq 50^\circ$. It is known that pure PEO has two well

defined reflection peaks at 2θ values 19.1° and 23.3° ^[3,16] while Pure PVA exhibits only a broad and shallow diffraction feature around the 2θ value of 20° ^[17-19]. Spectrum (3a), for undoped blend sample shows well defined broad peaks at around 19° and 23° , which are unique to the feature of PEO. These result reflect that PEO remain as separate phases with no significant mixing. However, XRD patterns (3b-3e) of blend sample doped with ZnO ≤ 5.0 wt% show two peaks at $2\theta = 19^\circ$ and 23° , which have been found to be increased in broadness and decreased in intensity. The reflection peaks of ZnO^[20] at 2θ values 31.7° , 34.4° and 36.2° begin to appear as small peaks and their intensity increase with increasing ZnO content. Above 5.0 wt% ZnO concentration spectrum (f) it was observed that the reflection of ZnO peaks disappeared which revealed that there is distortion in crystal structure of the blend. These results reveal the increase in amorphous content of the doped blend films with increasing the percentage of ZnO in the polyblend. The tendency of apparently diminution of crystallinity may be a result of dilution effect of ZnO when mixed with blend sample, which suppress recrystallization of broken polyblend polymer chains and inhibit crystal growth.

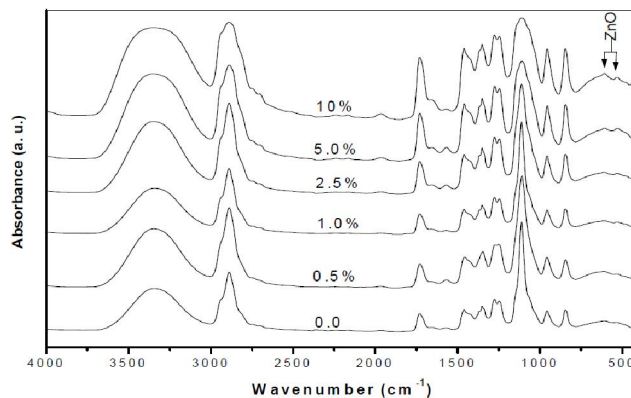


Figure 2 : FT-IR absorption spectra of (50/50wt/wt. %) PEO/PVA undoped blend and doped with different concentrations of ZnO nanoparticles (0.5, 1.0, 2.5, 5.0 and 10 wt %).

Ultraviolet-visible spectroscopy

UV-vis spectroscopy corresponds to electronic excitations between the energy levels related to the molecular orbital of the system. UV-vis spectra of all films are recorded at room temperature in the range of 200-800 nm as shown in Figure 4. PEO/PVA/nano-ZnO composites exhibit very small transmittance in the ultraviolet range (200-380 nm) while in visible range showed

Full Paper

very high transmittance. Consequently these materials are considered as an optically transparent in visible region which are easily manufactured by processes that do not utilize volatile organic compounds, and whose polymer components are not environmentally hazardous. The spectrum (4a) of undoped blend sample exhibited three absorption bands, an intense band at 210 nm and a humps at 280 and 340 nm, which are related to high energy absorption. The first band was associated with the presence of some residual acetate groups of PVA and/or chromophoric groups of PEO. While the humps at 280 and 340 nm were assigned to the existence of carbonyl groups associated with ethylene unsaturation^[21]. The bands at 280 and 340 nm may be due to $\pi \rightarrow \pi^*$ (K-band) and $n \rightarrow \pi^*$ (R-band) electronic transitions respectively. In addition, there are no absorption bands on the visible region for all samples under investigation since the films are transparent. The spectra (4b-4f) of blend samples doped with various concentrations of ZnO contain an additional band at 373 nm^[22], which can be assigned to ZnO chromophoric groups. The absorption intensity of this band increases with increasing ZnO wt% content in blend sample. The absorption intensity of the bands at 280 and 340 become faint at higher concentrations ≥ 2.5 ZnO wt%. However, only the peak position of the band at 210 nm shifted toward higher wavelengths by about 10 nm with increasing Zn-O concentrations. This shift indicates the complexation between the polyblend polymer and the filler takes place.

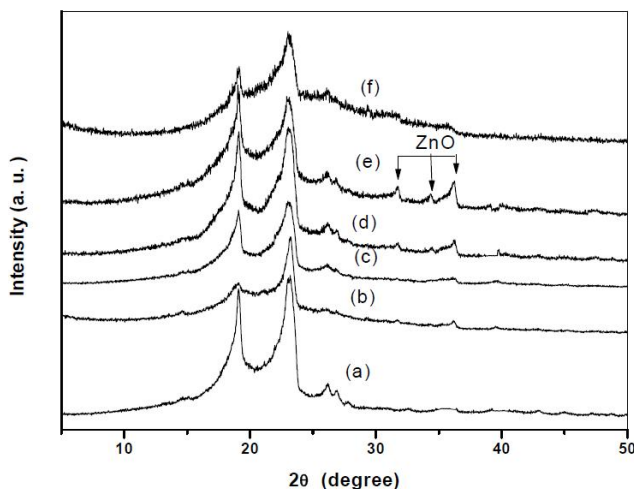


Figure 3 : X-ray diffraction of: a) undoped 50/50 (wt/wt. %) PEO/PVA undoped blend and doped with: b) 0.5, c) 1.0, d) 2.5, e) 5.0 and f) 10 wt. % ZnO nanoparticles.

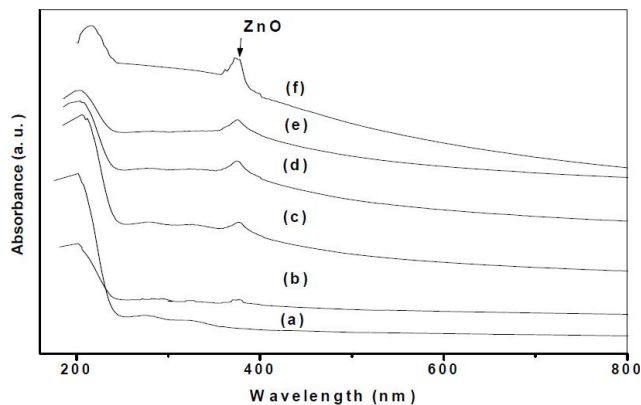


Figure 4 : UV-vis spectra of: a) undoped 50/50 (wt/wt. %) PEO/PVA undoped blend and doped with: b) 0.5, c) 1.0, d) 2.5, e) 5.0 and f) 10 wt. % ZnO nanoparticles.

The fundamental absorption edge is one of the most important feature of the absorption spectra of crystalline and amorphous materials. The nature of optical transition involved in the blends can be determined on the basis of the dependence of absorption coefficient (α) on photon energy ($h\nu$). The absorption coefficient (α) was calculated from the absorbance (A)^[21].

$$I = I_0 \exp(-\alpha x) \quad (1)$$

$$\text{Hence; } \alpha = \frac{2.303}{d} \log\left(\frac{I}{I_0}\right) = \frac{2.303}{d} A \quad (2)$$

Where I_0 and I are the intensities of incident and transmitted radiation respectively, d is the thickness of the sample.

Figure 5 shows the plot of absorption coefficient with photon energy for undoped blend films and doped with different concentration of ZnO. The extrapolation of the linear portion of the curves has been used to find the values of the absorption edge which are listed in TABLE 1. It is clear that the values of the absorption edge for doped PEO/PVA decreased as ZnO wt% increases. This may reflect the induced change in the number of available final states and/or the creation of localized states in the band gap as a result of compositional disorder^[23,24].

The transition occurs between extended states of band and localized states of the tail of the other band and the absorption coefficient (α) is given by the Urbach relation^[25]:

$$\alpha(\nu) = \alpha_0 \exp\left(\frac{h\nu}{E_c}\right) \quad (3)$$

where α_0 is a constant and E_c is the width of the tail of

the localized states in the band gap that associated with the amorphous nature of the materials. In general the larger the value of E_e , the greater in the structural disorder. Figure 6 shows the relation between $\ln \alpha$ and $h\nu$ for all investigated samples. The straight lines obtained suggest that the absorption follows the quadratic relation for inter-band transitions and the Urbach rule is obeyed. The values of band tails, E_e were calculated from the slope of the straight lines and are listed in TABLE 1. The tail states were generated due to disorder in the system^[13]. It is clear that values of the band tail increases with increasing the concentration of ZnO in blend system which confirming the increase in the disorder in such system.

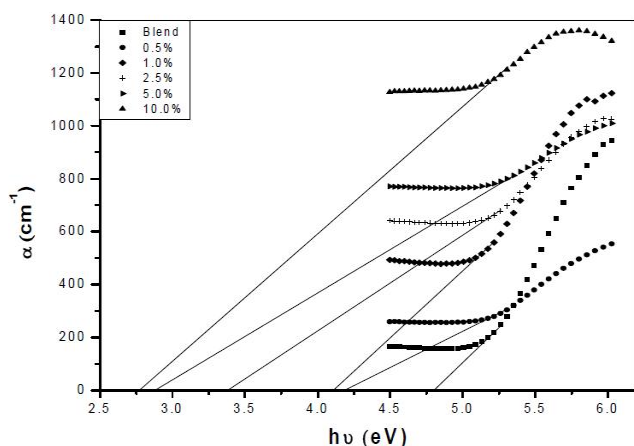


Figure 5 : The relation between absorbance coefficient (α) versus $h\nu$ for (■) Undoped blend, (●) 0.5, (◆) 1.0, (+) 2.5, (▶) 5.0, (▲) 10.0 wt% ZnO nanoparticles.

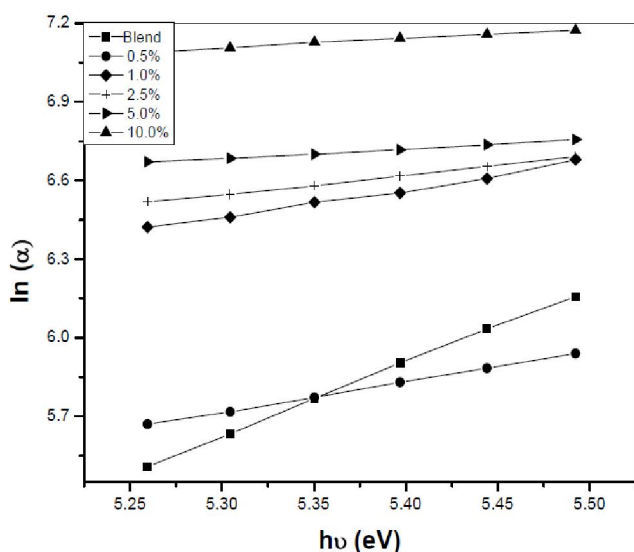


Figure 6: The relation between $\ln \alpha$ versus $h\nu$ for (■) undoped blend, (●) 0.5, (◆) 1.0, (+) 2.5, (▶) 5.0, (▲) 10.0 wt% ZnO nanoparticles.

TABLE 1 : The values of the absorption edge and band tail for undoped PEO/PVA and doped with different concentrations of ZnO nanoparticles.

ZnO Wt.%	Absorption edge (eV)	Band tail (eV)
0.0	4.79	0.35
0.5	4.20	0.86
1.0	4.10	0.92
2.5	3.37	1.33
5.0	2.86	2.73
10.0	2.70	2.77

Scanning electron microscopy (SEM)

SEM is used to investigate fully the effect of ZnO nanoparticles content and to examine the dispersion of nanocomposites particles in the polyblend polymer matrix.

Figure 7 shows typical SEM image of PEO/PVA blend without and with different concentrations of ZnO nanoparticles content. Image (a) for undoped polymer blend is found to be in a uniform morphology revealing a rather smooth surface. It is apparent that the addition of nano- ZnO particles in PEO/PVA polyblend exhibits changes in the surface morphology of such system (see images b- f). As the content of ZnO increases up to 2.5 wt% the film surface becomes roughness with some small particles (white spot) aggregates (see images b-d). This indicates segregation of ZnO in the polymeric matrixes and this may be confirmed the interaction and complexation between them. Also, this fact shown that a good adhesion between the surface of ZnO nanoparticles and polyblend polymer matrix has been established by the organic surface modification of the ZnO nanoparticles^[26]. Spots white on the backscattered images seem to be agglomerates of ZnO particles, which increase with increasing the concentration ZnO. Image (e) gives rise to crystalline domains with coarse spherulitic structure. This is due to ZnO segregated into inter-lamellar or intercrystalline regions of the blend. Image (f) shows smooth ganglia- like hills with some wrinkles (longitudinal shapes) of length about 5 μm , width 0.25-0.75 μm , and height \sim 1.2 μm ^[15]. This is attributed to a strong increase of lamellar twisting period and to a decreased radial growth rate in amorphous regions within the polymeric matrixes.

Differential scanning calorimetry (DSC)

DSC technique is the convenient tool to determine the physical and chemical changes such as glass transi-

Full Paper

tion temperatures (T_g), melting point (T_m), thermal decomposition temperature (T_d) in addition to the associated enthalpy for each process. DSC thermograms of PEO/PVA polymer blend and PEO/PVA/ZnO

nanocomposites films are shown in Figure 8. The values of glass transition temperature (T_g), melting temperature (T_{m1} and T_{m2}) and decomposition temperature (T_d) are recorded in TABLE 2.

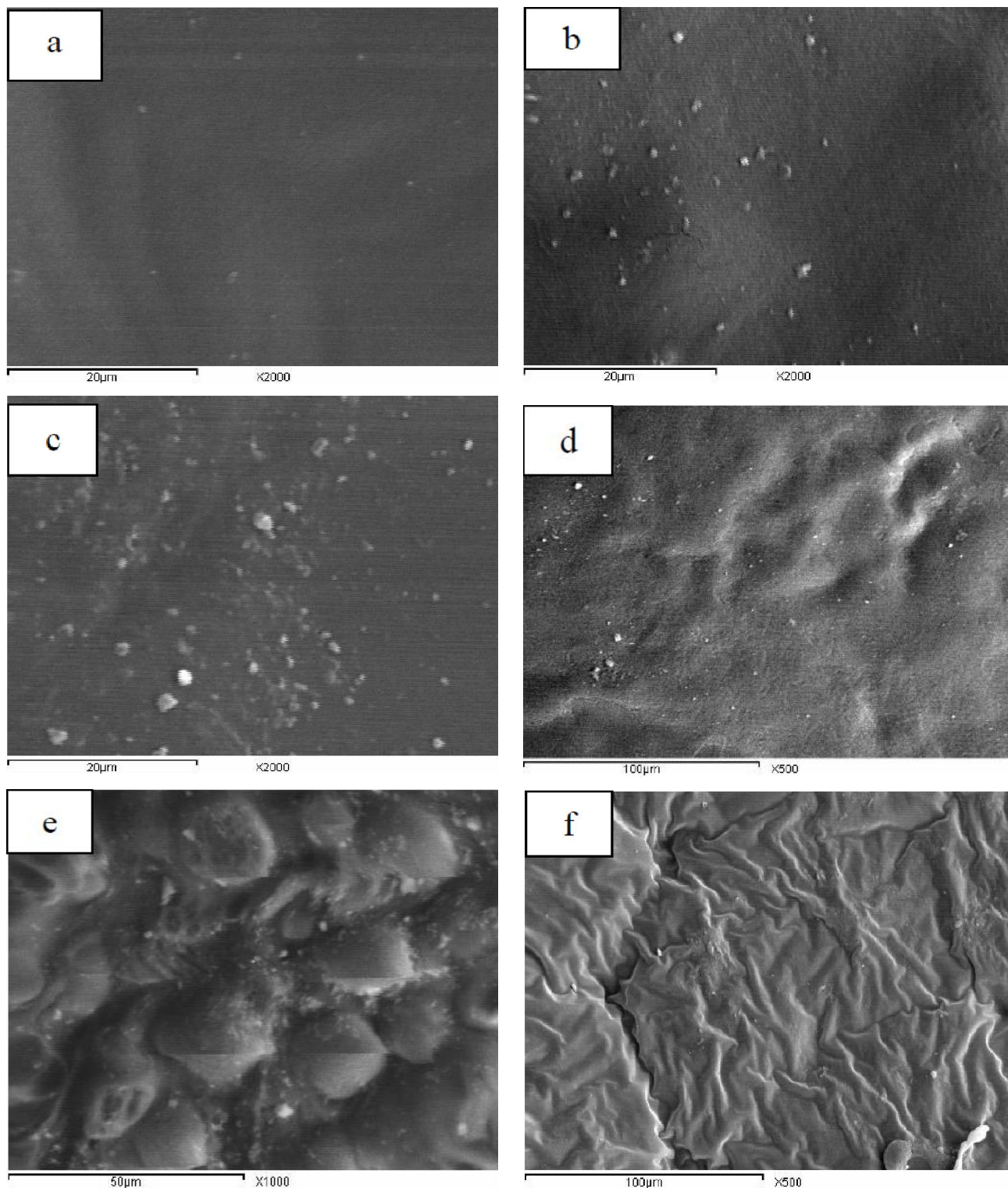


Figure 7 : SEM images of: a) PEO/PVA undoped blend and doped with: b) 0.5, c) 1.0, d) 2.5, e) 5 and f) 10 wt. % ZnO nanoparticles.

The DSC thermograms of all samples showed four endothermic peaks. The first endothermic peak at -34°C was assigned to T_{g1} of PEO. The second endothermic peak at 66°C was attributed to the overlapping of T_{m1} of PEO and T_{g2} of PVA. The third endothermic peak at 186°C was assigned to T_{m2} of PVA. The fourth endothermic peak T_d was observed in the range between 284 up to 310°C . It is reported previously^[27] that the glass transition temperature of the PVA was expected to be close to 71°C . Coincidentally, it was near the melting point of PEO, 66°C . Therefore, the glass transition peak of PVA might overlap with the melting peak of PEO in DSC thermogram and it could be difficult to observe the glass transition temperature separately. It is clear from TABLE 2 that the position of [T_{m1} of PEO & T_{g2} of PVA] and T_{m2} remains unaltered with increasing ZnO content in blend sample. While the position of T_d peak shifted to lower temperatures with increasing ZnO content in blend sample indicating to the decrease of thermal stability and weakening the bond strength. It is generally accepted that the presence of two separate T_g 's in polymer blends provides a strong signature of immiscibility. Immiscible blends may be further described as compatible or incompatible. In the present case, the blend sample of PEO/PVA undoped and doped with ZnO nanoparticles are immiscible but still compatible.

To understand the change in the structural characteristic induced by adding ZnO nanoparticles, the degree of crystallinity χ_c for PVA was measured from the heat of fusion at melting for PVA by the following equation^[28]

$$\chi_c = \frac{\Delta H_f}{\Delta H_{f(100)}} \times 100 \quad (4)$$

where ΔH_f is the heat of fusion of PVA; $\Delta H_{f(100)}$ is the heat of fusion of 100% crystallinity of pure PVA ($\Delta H_{f(100)} = 160 \text{ Jg}^{-1}$)^[1]. Since T_g of PVA is overlapped with T_m of PEO, so it is difficult to determine exactly the enthalpy associated with melting point of PEO. Thus, the calculation of the change in the degree of crystallinity for PEO with increasing ZnO concentrations is not preferable. The estimated values of the degree of crystallinity for the PVA after adding ZnO to blend film are tabulated in TABLE 2.

It is clear from TABLE 2 that there is a decrease in

the degree of crystallinity after the addition of different concentration of ZnO for all samples. This behaviour reflects that the addition of ZnO to the PEO/PVA sample decreases the intermolecular interaction and/or crosslinking PEO and PVA components. This result is consistent with that previously obtained data from XRD patterns and band tail width for such blend system.

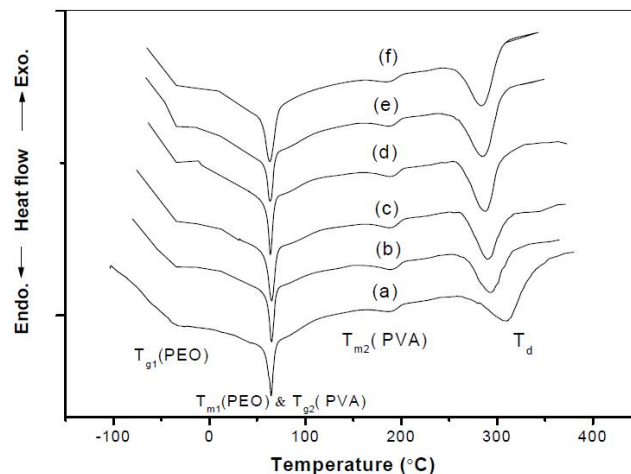


Figure 8 : DSC of: a) undoped PEO/PVA blend and doped with: b) 0.5, c) 1.0, d) 2.5, e) 5 and f) 10 wt. % ZnO nanoparticles.

TABLE 2 : The values of [T_{m1} (PEO) & T_{g2} (PVA)], T_{m2} , T_d and χ_c (PVA) for undoped PEO/PVA and doped with different concentration of ZnO nanoparticles.

ZnO Wt.%	T_{m1} (PEO) & T_{g2} (PVA) ($^{\circ}\text{C}$)	T_{m2} ($^{\circ}\text{C}$)	T_d ($^{\circ}\text{C}$)	χ_c (%)
0.0	64	188	310	9.70
0.5	65	189	294	9.30
1.0	65	190	292	9.10
2.5	64	189	288	9.05
5.0	63	187	285	9.00
10	63	186	284	7.50

Thermogravimetric analysis (TGA) and its derivative (Dr TG)

Thermogravimetric analysis is a process in which substance is decomposed in the presence of heat which causes bonds within the molecules to be broken. The sample weight decreases slowly as the reaction begins, then decreases rapidly over a comparatively narrow temperature range and finally levels off as the reactants become spent. The shape of TGA curve depends primarily upon the kinetics parameters^[29].

Figure 9 shows TGA thermograms and Dr TG as a function of temperature in the range from 20°C to 460

Full Paper

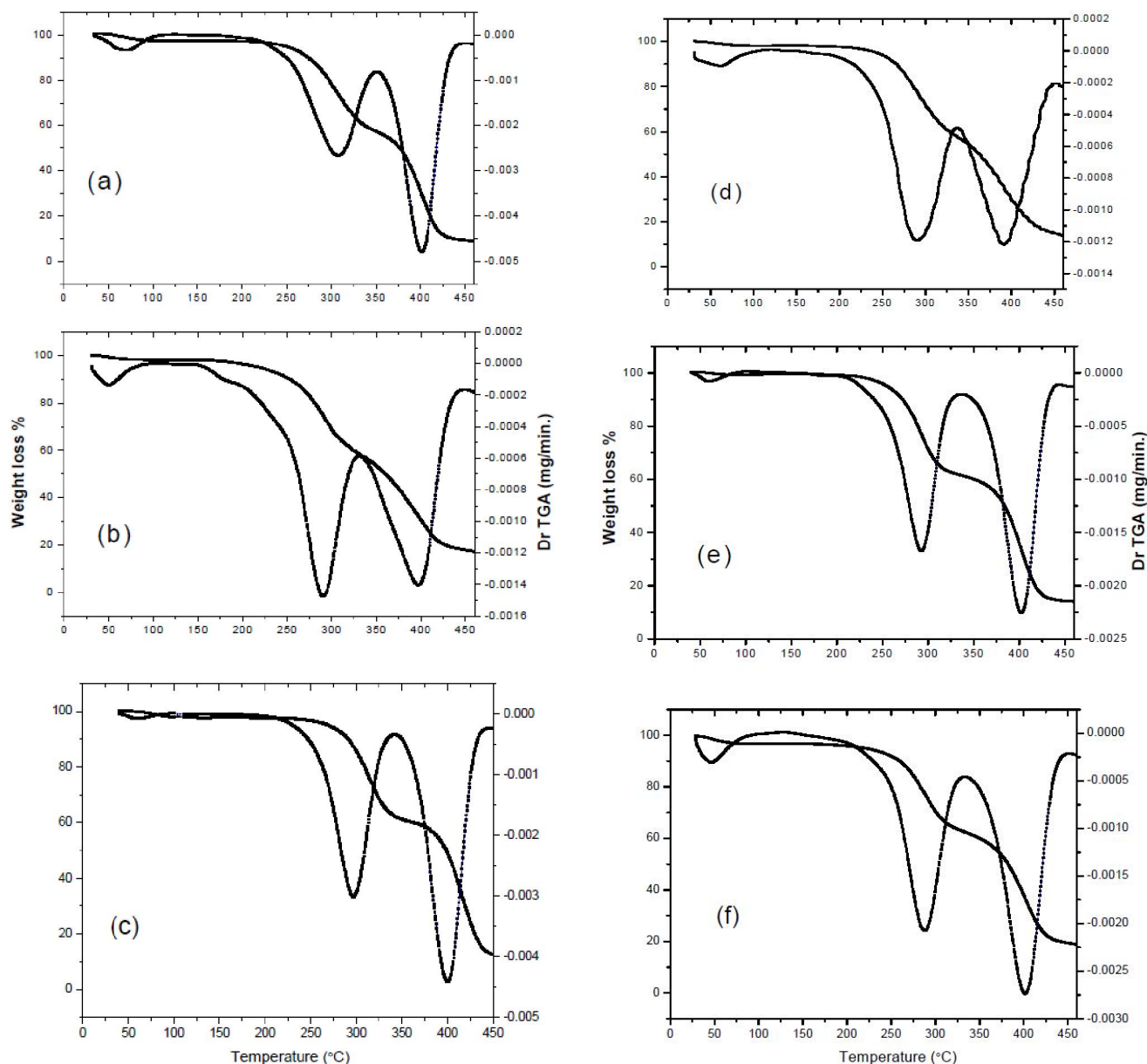


Figure 9 : TGA & Dr TGA of : a) undoped PEO/PVA blend and doped with : b)0.5, c)1.0, d)2.5, e)5.0, f) 10 wt.% ZnO nanoparticles.

°C for PEO/PVA blend undoped and doped with different concentrations of ZnO nanoparticles. It is clear from Figure 9 that all samples have three steps of decomposition. TABLE 3 represents the decomposition steps and percentage weight loss for PEO/PVA blend undoped and doped with different concentration of ZnO nanoparticles. The lower values of percentage weight loss, in the first decomposition step which include the melting point of PEO (0.88-3.00 %) may be due to splitting or volatilization of small molecule, and/or the evaporation of moisture. The second decomposition region in TG curves which cover a wider

temperature range including the melting point of PVA have a percentage weight loss (35.0- 40.0 %). The latter process in TG curves which is the main decomposition step have a more significant percentage weight loss (43.0-50.0 %).

The difference in thermal decomposition behaviour of the investigated samples can be seen more clearly from curves shown in Figure 9. DrTG curves show three temperature broad peaks T_p 's corresponding to the three decomposition regions (see TABLE 3). It is noted that the peak temperature T_p of DrTG curves blend sample doped with various ZnO content in all regions are shifted

to lower temperatures compared to undoped blend sample. This indicates that the thermal stability of blend sample decreases by mixing it with ZnO nanoparticles.

TABLE 3 : TG and Dr TG data for undoped PEO/PVA and doped with different concentration of ZnO nanoparticles.

ZnO Wt.%	Region of Decomposition	Temperature(C°)			Weight loss (%)	
		Start	End	Tp	Partial	Total
0.0	1 st	38	115	69	3.00	92.0
	2 nd	162	348	309	40.0	
	3 rd	348	460	401	49.0	
0.5	1 st	32	67	50	1.50	88.5
	2 nd	132	313	290	44.0	
	3 rd	314	426	397	43.0	
1.0	1 st	34	97	59	2.40	88.4
	2 nd	197	329	297	36.0	
	3 rd	330	445	400	50.0	
2.5	1 st	31	82	62	2.00	82.0
	2 nd	177	326	291	37.0	
	3 rd	327	433	392	43.0	
5.0	1 st	40	105	60	0.90	86.0
	2 nd	181	320	293	36.0	
	3 rd	320	453	402	49.0	
10	1 st	31	116.4	47	3.00	81.0
	2 nd	156	336.2	288	35.0	
	3 rd	336	455.1	402	43.0	

Tp*: Peak temperature of DrTGA

The thermodynamics activation parameters of the decomposition process were evaluated by making use of the well known Coats- Redfern equation^[30] for first order reaction in the form:

$$\ln\left[\frac{-\ln(1-\delta)}{T^2}\right] = -\frac{E^*}{RT} + \ln\frac{AR}{\beta E^*} \quad (5)$$

where A is constant, β is heating rate, R is the universal gas constant, δ is fraction of decomposition and E^* is

the activation energy. Therefore plotting $\ln\left[\frac{-\ln(1-\delta)}{T^2}\right]$

against $1/T$ according to equation (5) (Figure not shown for sake brevity) should give a straight line whose slope

is directly proportional to the activation energy ($-\frac{E^*}{R}$).

The activation entropy ΔS^* , the activation enthalpy ΔH^* , and the free energy (Gibbs function ΔG^*) were calculating using the following equations^[31]:

$$\Delta S^* = 2.303 \left[\log \frac{Ah}{kT} \right] R \quad (6)$$

$$\Delta H^* = E^* - RT \quad (7)$$

$$\Delta G^* = \Delta H^* - T\Delta S^* \quad (8)$$

where k and h are Boltzmann and Planck constants respectively, T is the temperature involved in the calculation selected as the peak temperature of DrTG. The entropy ΔS^* gives information about the degree of order of the system, the enthalpy ΔH^* gives information about the total thermal motion and Gibbs or free energy ΔG^* gives information about the stability of the system.

TABLE 4 : Thermodynamic parameters for undoped PEO/PVA blend and doped with different concentrations of ZnO nanopowder.

ZnO Wt.%	E*(kJ/mole)		$\Delta S^*(J/K.mole)$		$\Delta H^*(kJ/mole)$		$\Delta G^*(kJ/mole)$	
	2 nd region	3 rd region						
0.0	101	159	-82	-27	98	156	123	166
0.5	122	139	-31	-45	120	136	128	154
1.0	122	164	-40	-11	120	160	131	165
2.5	125	142	-30	-43	123	139	132	156
5.0	130	162	-21	-16	127	159	133	165
10	132	166	-12	-9	130	163	134	166

According the Coats- Redfern method the calculated thermodynamic parameters values are given in TABLE 4. It is clear that the values of ΔH^* , ΔG^* and ΔS^* in the second decomposition step increase with increasing ZnO concentration in blend sample except that ΔS^* at 1.0 wt% ZnO decreases but still higher than the undoped one. This result indicates that the addition of ZnO to PEO/PVA blend sample cause an increase of thermal motion and a decrease of both thermal stability and the ordered of such system. However, in the third decomposition step the values of ΔH^* , ΔG^* and ΔS^* for most doped blend samples are lower than the undoped sample and change irregularly with increasing ZnO concentrations. Also, it is to be mentioned that the values of ΔH^* and ΔG^* in the second decomposition step are less than those of the third decomposition step while ΔS^* shows irregular trend. Comparing these results, it can be concluded that the nature of the second decomposition region is relatively low thermal motion, more orderness and relative thermal stability of most samples with respect to the third decomposition process.

Full Paper

The activation energies for this system are small at second stages of degradation and high at the third stages. These lower values are most likely associated with process that occurs at weak linkage of PEO/PVA/ZnO system. By increasing the temperature, random scission of macromolecular chains predominates and the activation energy has a greater value.

CONCLUSIONS

Although the blend films undoped and doped with ZnO formed were homogenous, coherent and showed neither separation into bilayers nor any precipitation; IR and DSC data reveal that they are immiscible. The presence of ZnO in PEO/PVA blend sample induce a decrease of crystallinity as indicated by XRD and UV-visible which is also confirmed from heat of fusion in DSC thermograms. TG data provide that thermal stability decrease as a result of addition of ZnO nanoparticles to polyblend system. As the content of ZnO increases in the polyblend sample, the surface morphology becomes roughness with white spot and it reveals the tendency towards phase segregation in the interlamellar or intercrystalline regions of the polyblend chain.

Finally, it can be concluded that the film properties can be significantly modified by incorporation of nano-ZnO at a concentration ≤ 5.0 wt% in blend sample. At higher proportions of nano-ZnO resulting in agglomeration of ZnO particles and deterioration in film properties.

REFERENCES

- [1] L.Z.Zhang, Y.Y.Wang, C.L.Wang, H.Xiang; *J.Membr.Sci.*, **308**, 198 (2008).
- [2] M.Abdelaziz; *Physica B*, **406**, 1300 (2011).
- [3] K.K.Kumar, M.Ravi, Y.Pavani, S.Bhavani, A.K.Sharma, V.V.R.N.Rao; *Physica B*, **406**, 1706 (2011).
- [4] D.A.J.Rand; *J.Power Sour.*, **4**, 101 (1979).
- [5] G.Momen, M.Farzaneh; *Rev.Adv.Mater.Sci.*, **27**, 1 (2011).
- [6] B.Erdem, E.D.Sudol, V.L.Dimonie, M.El-Aasser; *J.Polym.Sci.Polym.Chem.*, **38**, 365 (2000).
- [7] A.A.Khan, A.M.Mezbaul; *React.Func.Polym.*, **55**, 277 (2003).
- [8] H.Kawaguchi; *Prog.Polym.Sci.*, **25**, 1171 (2001).
- [9] F.B.Xing, G.X.Cheng, B.X.Yang, L.R.Ma; *J.Appl.Polym.Sci.*, **91**, 2669 (2004).
- [10] E.Tang, G.Cheng, X.Pang, X.Ma, F.Xing; *Colloid Polym.Sci.*, **284**, 422 (2006).
- [11] J.Lee, D.Bhattachanya, A.J.Easteal, J.B.Metson; *Current.Appl.Phys.*, **8**, 42 (2008).
- [12] R.Mishra, K.J.Rao; *Eur.Polym.J.*, **35**, 1883 (1999).
- [13] A.M.Shehap; *Egypt.J.Solids*, **31**, 1 (2008).
- [14] S.Ramesh, T.F.Yuen, C.J.Shen; *Spectrochimica Acta Part A*, **69**, 670–675 (2008).
- [15] Y.Wang, X.Fan, J.Sun; *Mater.Lett.*, **63**, 350 (2009).
- [16] U.Sasikala, P.Naveen Kumar, V.V.R.N.Rao, A.K.Sharma; *International Journal Of Engineering Science& Advanced Technology*, **2**, 722 (2012).
- [17] N.Ahad, E.Saion, E.Gharibshahi; *Journal of Nanomaterials*, (2012).
- [18] E.Saion, M.A.M.Teridi; *Ionics*, **12**, 53 (2006).
- [19] M.Abdelaziz, M.M.Ghannam; *Physica B*, **405**, 958 (2010).
- [20] B.Wen, Y.Huang, J.J.Boland; *J.Phys.Chem.C*, **112**, 106 (2008).
- [21] E.M.Abdelrazek, I.S.Elashmawi, A.El-Khodary, A.Yassin; *Current Appl.Phys.*, **10**, 607 (2010).
- [22] Y.Gui, S.Li, J.Xu, C.Li; *Microelectronics J.*, **39**, 1120 (2008).
- [23] N.F.Molt, E.A.Davis; *Electronic processes in nancrystalline materials*, and ed., Oxford University Press : Oxford, 273 (1979).
- [24] F.H.Abd El-Kader, S.A.Gafer, A.F.Basha, S.J.Bannon, M.A.F.Basha; *J.Polym.Sci.*, **118**, 413 (2010).
- [25] F.Urbach; *Phys.Rev.*, **92**, 1324 (1953).
- [26] A.Matei, I.Cernica, O.Cadar, C.Roman, V.Schiopu; *Int.J.Mater.*, **11**, 767 (2008).
- [27] W.C.Lai, W.B.Liau; *J.Appl.Polym.Sci.*, **92**, 1562 (2004).
- [28] O.W.Guirguis, M.T.H.Moselhey; *Natural Science* **4**, 57-67 (2012).
- [29] R.Silva, G.M.Carvalho, E.C.Muniz, A.F.Rubira; *Polímeros*, **20**, 153 (2010).
- [30] A.W.Coats, J.P.Redfern; *Nature*, **201**, 68 (1964).
- [31] F.Yakuphanoglu, A.O.Gorgulu, A.Cukurovali, *Physica B*, **353**, 223 (2004).